

Comparing Lassoing Criteria and Modeling Straight-line and One-loop Lassoing Motions Considering Criteria

Hiroki Usuba
Meiji University
Nakano-ku, Japan
m@mimorisuzu.co

Shota Yamanaka
Yahoo Japan Corporation
Chiyoda-ku, Japan
syamanak@yahoo-corp.jp

Homei Miyashita
Meiji University
Nakano-ku, Japan
homei@homei.com

ABSTRACT

In graphical user interfaces, users can select multiple objects simultaneously via lasso selection. This can be implemented, for example, by having users select objects by looping around their centers or entire areas. Based on differences in lassoing criteria, we presume that the performance of the criteria also differs. In this study, we compare three lassoing criteria and model lassoing motions while considering these criteria. We conducted two experiments; participants steered through straight-line and one-loop paths by using three criteria. The participants handled the lassoing criteria correctly and performed lassoing at appropriate speeds for each path shape. Although the drawn trajectories varied depending on the lassoing criteria, the criteria in the performance and subjective evaluations did not differ significantly. Additionally, from our results, we build a baseline model to predict the movement time by considering the lassoing criteria. We also discuss further experiments to predict movement time under more complex conditions.

Author Keywords

Lasso criteria; multiple selection; steering law; graphical user interfaces.

CCS Concepts

•Human-centered computing → Graphical user interfaces; HCI theory, concepts and models;

INTRODUCTION

Creating a selection range is a fundamental operation in graphical user interfaces (GUIs). For example, when users want to move multiple objects at the same time, they create a selection range containing the desired objects. In desktop interfaces, file explorers, and photo managers, objects are arranged on a grid. Thus, users use rectangle-based selection. In illustration and note-taking applications, in which objects exist in various locations, *lassoing* is another option. Lassoing allows users to draw a stroke freely and thus select objects in a selection range that they draw. In current GUIs, there are various ways

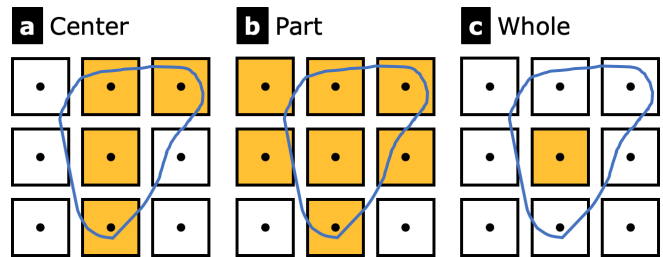


Figure 1. Yellow objects selected using lasso with different selection criteria, even though lasso stroke is same. (a) *Center*: Objects whose centers are inside stroke. (b) *Part*: Objects fully inside or crossed by stroke. (c) *Whole*: Objects whose entire areas are inside stroke.

to implement lassoing, including the following three examples illustrated in Figure 1.

- *Center* denotes the circling selections [10]. In this operation, objects whose centers are within the selection range are selected (Figure 1a).
- *Part* denotes the selection of objects that are partially within the selection range (Figure 1b), e.g., in Adobe Illustrator CC.
- *Whole* denotes the selection of objects that are completely within the selection range (Figure 1c), e.g., in Microsoft OneNote.

For this study, we chose *Whole* and *Part* because they are widely equipped in major applications. In addition, we chose *Center*, which has been cited in many papers on target selection, one of the main topics of lassoing.

As shown in Figure 1, even if users draw the same stroke by using different lassoing criteria, the objects to be selected differ. The reason is that the path through which users can actually steer depends on the lassoing criteria. For example, when users want to select 2×2 objects that are in the center of 4×4 objects, the paths that users can take for each criterion are as shown in Figure 2. The path width is the same between the lassoing criteria; however, the path amplitude differs; it is short in the order of *Part*, *Whole*, and *Center*. Thus, as based on the steering law [1], by using *Part*, whose path amplitude is the shortest, it is estimated that users can operate the fastest. Existing studies [6, 8, 10, 15] on selecting multiple objects focus on comparing one lassoing criterion and other selection techniques. That is, as mentioned above, many lassoing criteria are implemented in current applications, whereas it is unclear which criteria should be adopted in illustration applications for example.

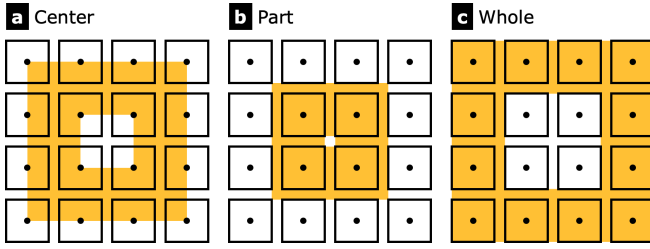


Figure 2. Visualizing path through which user can actually steer with each lasso selection method: (a) *Center*, (b) *Part*, and (c) *Whole*. User can select 2×2 objects at center by passing through yellow-highlighted path for each criterion.

In addition to comparing methods of selecting multiple objects, modeling lassoing motions has been conducted. For example, Yamanaka et al. modeled steering through successive objects [17] and lassoing motion in a grid of icons [16]. However, in their studies, users could not touch any of the objects when performing lassoing operations. As shown in Figure 2, when using *Center* for example, users can steer between the centers of the objects, and, with other lassoing criteria, they can perform operations while touching objects. Thus, Yamanaka et al.’s lassoing model does not consider lassoing criteria. Additionally, if considering lassoing criteria, increasing the interval between objects and the size of objects would increase not only the path width but also the path amplitude. That is, in their studies, the effects of the factors involved in lassoing operations were not investigated under the consideration of lassoing criteria.

In this study, we conducted two experiments in which participants steered through straight-line (Figure 4b) and one-loop paths (Figure 15a) by using the three criteria. The lassoing operations consisted of steering through a straight-line path and turning at a corner. In the straight-line path task, because the path amplitude is controlled, increasing the interval between objects does not increase the path amplitude. That is, with the task, we believe that it is possible to find the pure effects of the factors involved in lassoing operations when using different criteria. In the one-loop path task, users must turn at corners in order to enclose the targets. By conducting these two experiments, we clarified the basic performance of the lassoing criteria. In addition, modeling steering through a path with corners on the basis of the criteria meant succeeding in building a baseline model. Our key contributions are as follows:

- We compared the lassoing criteria and conducted lassoing tasks while considering the criteria for the first time.
- Our results showed that there were no significant differences in the movement time, error rate, and subjective evaluation between the lassoing criteria.
- We succeeded in building a baseline model; the steering law can sufficiently predict the movement time of lassoing motion even in consideration of the criteria.

RELATED WORK

Selecting Multiple Objects

Methods for selecting multiple objects have been developed. Mizobuchi et al. proposed the circling selections [10] by which

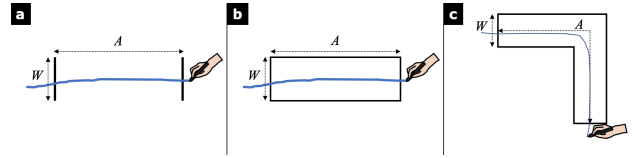


Figure 3. Example of (a) crossing operations, (b) steering operations, (c) steering at corner.

users can select objects whose centers are in the selection range (Figure 1a). They also found that the circling selections is generally slower and less accurate than tapping. Dehmeshki et al. proposed *PerSel* and compared this method with lassoing and rectangle selection methods [6]. Their experiment showed that that lassoing selection is the fastest among the methods. In addition, other selection methods [8, 15] have been developed and compared with lassoing selection. In summary, many researchers focus on not comparing lassoing criteria but rather proposing new selection methods (and comparing the methods and the lassoing selection).

Modeling Steering and Lassoing Motions

Fitts’ law (Equation 1) is a model for predicting the movement time (MT) taken when selecting a target with width (W), distance (A), and two regression constants (a and b_p) [7]. The two-goal passing task (Figure 3a), which is called *crossing*, can be modeled with the same equation [1]. Let the goals’ length be W and distance be A .

$$MT = a + b_p \log_2 \left(\frac{A}{W} + 1 \right) \quad (1)$$

When the distance between the two goals is filled by other goals, i.e., users pass through infinite goals without intervals, the task becomes *steering* (Figure 3b). Examples of steering operations include navigating hierarchical menus and lassoing. The steering law [1] is derived from the integral of Equation 1 and is as follows:

$$MT = a + b_s ID, \text{ where } ID = \frac{A}{W} \quad (2)$$

where A denotes the path amplitude, W is the path width, and b_s is a regression constant.

When users steer through a path with a corner (Figure 3c), the movement at the corner becomes a “stop and go” motion [11], i.e., the speed at the corner decreases sharply. Then, the steering law is modified by adding Fitts’ term as follows:

$$MT = a + b_s \frac{A}{W} + b_p \log_2 \left(\frac{A/2}{W} + 1 \right) \quad (3)$$

Yamanaka et al. modeled steering through successive objects [17] and lassoing motion in a grid of icons [16]. They found that the size of the interval between objects affects users’ movement. For example, when the interval is wide, the movement becomes a series of successive crossing motions, and, when it is narrow, the movement is a steering motion [17]. In addition, they showed that the movement time taken for the lassoing motion can be predicted by using a model that combines the steering law and Fitts’ law [16].

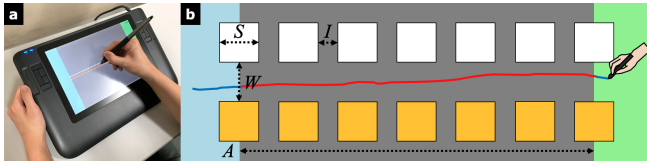


Figure 4. (a) Apparatus. (b) Experiment 1 task outline: participants had to steer through margin between targets and non-targets.

EXPERIMENT 1: STRAIGHT-LINE PATH

We conducted a task (Figure 4b) in which participants steered through a straight-line path because we wanted to investigate the pure effects of the factors (e.g., the path amplitude, interval between objects) involved in lassoing operations when using different criteria.

Apparatus

We used an Apple MacBook Pro laptop (Intel Core i5, 2.4 GHz, two cores, Intel Iris 1536 MB, 8 GB of RAM, macOS Sierra). The input device and display consisted of a Wacom Cintiq 12WX DTZ-1200 W IPS liquid crystal pen tablet (12.1 in., 261.1×163.2 mm, $1,280 \times 800$ pixels, Figure 4a). The full-screen experimental system was developed with JavaScript and allowed participants to interact with the screen through touch input by using a stylus (the screen did not register finger touching).

Participants

Twelve paid volunteers participated in this study (three women, nine men; age: $M = 23.67$, $SD = 1.55$ years). All participants were right-handed and operated the stylus accordingly. Each participant received 18 US\$ for the study. This experiment was conducted on a different day from Experiment 2.

Task

The task included a blue start area, white non-targets, yellow targets, and a green end area (Figure 4b). The center of the path was at the center of the screen. The participants were asked to draw a stroke to enclose all targets as quickly and accurately as possible from the start area to the end area. The stroke was displayed on the screen in blue until the start area was exited, in red along the path, and again in blue after the end area was entered [2]. After completing the stroke, the system created a selection range by combining the participant's red stroke and end points at the bottom of the screen, and if all targets were within the selection range and all non-targets were outside it, a "success" sound was played. Otherwise, a "failure" sound was played, and the trial was regarded as an error. In that case, the same task was added to the end of the remaining tasks and reattempted by the participant. After playing either sound, the system changed the colors of the target and non-target borders and displayed those selected and not selected. We asked the participants to confirm whether the trial was a success or a failure; if they did not understand why a trial was considered an error, we instructed them to ask about it. After confirming the trial result, the participants clicked a button and proceeded to the next trial. Consistent with other steering law studies [3, 17], if a participant lifted the stylus from the screen, a failure sound was played, but the trial was

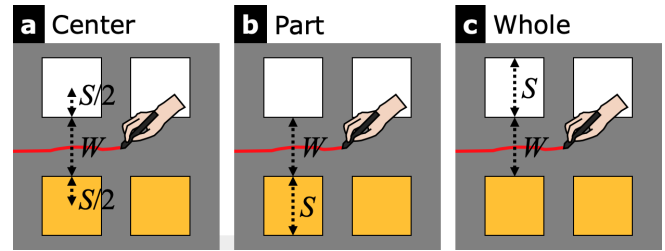


Figure 5. For each criterion, tolerance shifts, but width remains same (equal to $S + W$): (a) *Center*, (b) *Part*, and (c) *Whole*.

not regarded as an error, and the participant was instructed to redo it. To fairly compare all of the lasso criteria, the object centers were not displayed.

Design

The path amplitude A was 480 or 1000 pixels (97.73 or 203.61 mm, respectively). The object size S was 8, 12, 16, or 24 pixels (1.63, 2.44, 3.26, or 4.89 mm, respectively). The vertical margin W between the targets and non-targets was 14, 22, 30, or 44 pixels (2.85, 4.48, 6.11, or 8.96 mm, respectively). The horizontal interval I between two successive objects was always 10 pixels (2.04 mm), and thus, we believe that the participants always performed visually-controlled steering motions [17]. Three lasso criteria *Lasso* were considered: *Center*, *Part*, and *Whole* (Figure 1). Figure 5 shows that there was no difference in tolerance among the criteria. Targets and non-targets of a particular size (S) and interval (I) were distributed along the path amplitude A . The numbers of targets and non-targets along the path depended on A , S , and I ; thus, A was independent of S and I .

Procedure

The order of working with different criteria *Lasso* was balanced among the 12 participants through a Latin square pattern, and the orders of A , S , and W were randomized. One *set* consisted of $2A \times 4S \times 4W = 32$ trials. Before starting, each participant was briefed about the experiment and lasso selection. For each *Lasso*, after an introductory practice set, each participant completed five sets to produce experimental data. After completing all of the sets, we asked each participant what they expected with each lasso selection method. A total of 5,760 trials (i.e., $3Lasso \times 2A \times 4W \times 4S \times 5$ sets \times 12 participants) were conducted, which required approximately 30 min. per participant. We asked the participants to take a break if necessary.

Measurements

The dependent variables included the movement time MT (the time from exiting the start area to entering the end area, excluding error trials), the error rate, SD_y (the standard deviation of the trajectory's y-coordinate, including error trials), and M_y (the mean of the trajectory's y-coordinate, including error trials). Regarding the y-coordinate, the center of the screen was taken as zero, with $M_y > 0$ implying that the participant drew a stroke below the center.

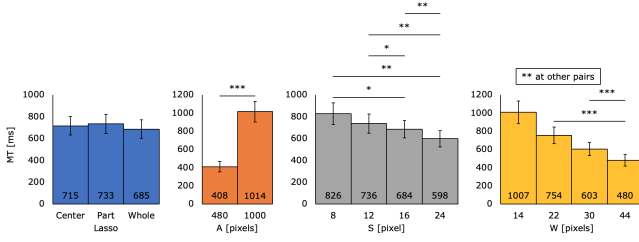


Figure 6. MT vs. L, A, S, and W.

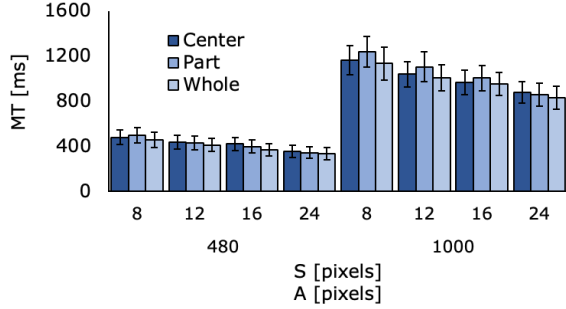


Figure 7. MT for $Lasso \times A \times S$.

Results

Among the 5,988 trials¹, 238 errors occurred (3.97%). We analyzed the data by using repeated-measures analysis of variations (ANOVA) and a Bonferroni post-hoc test. The independent variables were *Lasso*, *A*, *S*, and *W*, and the dependent variables were the same as those used in the measurements. In our graphs of the results, the error bars represent the standard error, and ***, **, and * indicate $p < 0.001$, $p < 0.01$, and $p < 0.05$, respectively.

Movement Time

We observed the main effects for *A* ($F_{1,11} = 104.81$, $p < 0.001$, $\eta_p^2 = 0.91$), *S* ($F_{3,33} = 18.07$, $p < 0.001$, $\eta_p^2 = 0.62$), and *W* ($F_{3,33} = 33.75$, $p < 0.001$, $\eta_p^2 = 0.75$) but not that for *Lasso* ($F_{2,22} = 1.57$, $p = 0.23$, $\eta_p^2 = 0.12$). Figure 6 shows the results of the post-hoc test. We also observed the interactions for $A \times S$ ($F_{3,33} = 16.96$, $p < 0.001$, $\eta_p^2 = 0.61$), $A \times W$ ($F_{3,33} = 63.54$, $p < 0.001$, $\eta_p^2 = 0.85$), $S \times W$ ($F_{9,99} = 15.91$, $p < 0.001$, $\eta_p^2 = 0.59$), $S \times A \times W$ ($F_{9,99} = 7.69$, $p < 0.001$, $\eta_p^2 = 0.41$), and $Lasso \times A \times S$ ($F_{6,66} = 2.36$, $p < 0.05$, $\eta_p^2 = 0.18$). Regarding all interactions, similar relationships to the relationship between the amplitude and width seen in the steering law tasks [1, 3] were found. In particular, for $Lasso \times A \times S$, as shown in Figure 7, there were no significant differences between *Lasso*.

Error Rate

We observed the main effects for *A* ($F_{1,11} = 19.77$, $p < 0.001$, $\eta_p^2 = 0.64$), *S* ($F_{3,33} = 7.17$, $p < 0.001$, $\eta_p^2 = 0.39$), and *W* ($F_{3,33} = 17.43$, $p < 0.001$, $\eta_p^2 = 0.61$) but not that for *Lasso* ($F_{2,22} = 0.28$, $p = 0.76$, $\eta_p^2 = 0.02$). Figure 8 shows

¹The data of ten successful trials was lost because of an experimental system error.

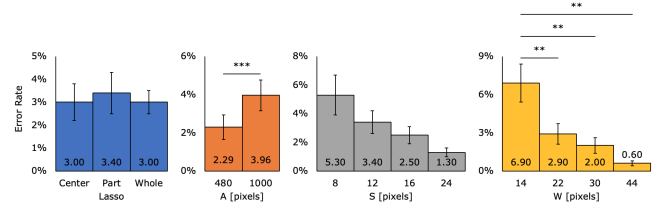


Figure 8. Error rate vs. L, A, S, and W.

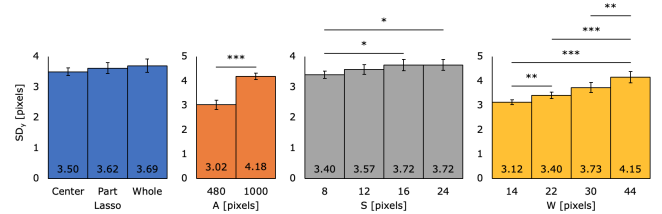


Figure 9. SD_y vs. L, A, S, and W.

the results of the post-hoc test. We also observed the interactions for $S \times W$ ($F_{9,99} = 2.96$, $p < 0.01$, $\eta_p^2 = 0.21$) and $Lasso \times A \times S \times W$ ($F_{18,198} = 1.82$, $p < 0.05$, $\eta_p^2 = 0.14$). Regarding $S \times W$, increasing *S* and/or *W* decreased the error rate. Regarding $Lasso \times A \times S \times W$, there were no significant differences between *Lasso*.

Standard Deviation of Y-coordinate

We observed the main effects for *A* ($F_{1,11} = 150.05$, $p < 0.001$, $\eta_p^2 = 0.93$), *S* ($F_{3,33} = 8.23$, $p < 0.001$, $\eta_p^2 = 0.43$), and *W* ($F_{3,33} = 29.03$, $p < 0.001$, $\eta_p^2 = 0.73$) but not that for *Lasso* ($F_{2,22} = 0.87$, $p = 0.43$, $\eta_p^2 = 0.07$). Figure 9 shows the results of the post-hoc test. We also observed the interactions for $A \times W$ ($F_{3,33} = 8.74$, $p < 0.001$, $\eta_p^2 = 0.44$), $Lasso \times A \times S$ ($F_{6,66} = 2.33$, $p < 0.05$, $\eta_p^2 = 0.17$), and $Lasso \times A \times W$ ($F_{6,66} = 3.21$, $p < 0.01$, $\eta_p^2 = 0.23$). Regarding $A \times W$, increasing *A* and/or *W* increased SD_y . Regarding $Lasso \times A \times S$ and $Lasso \times A \times W$, there were no significant differences between *Lasso* except where shown in Figure 10.

Mean of Y-coordinate

We observed the main effects for *Lasso* ($F_{2,22} = 118.43$, $p < 0.001$, $\eta_p^2 = 0.92$) and *A* ($F_{1,11} = 7.28$, $p < 0.05$, $\eta_p^2 = 0.40$)

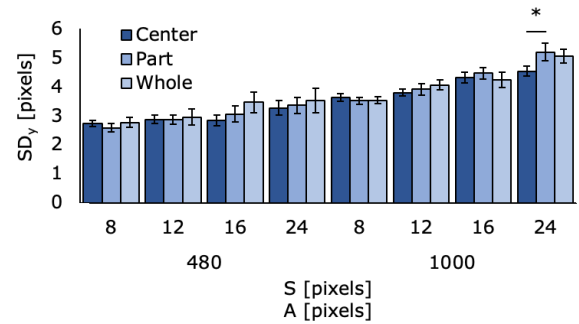


Figure 10. SD_y for $Lasso \times A \times S$.

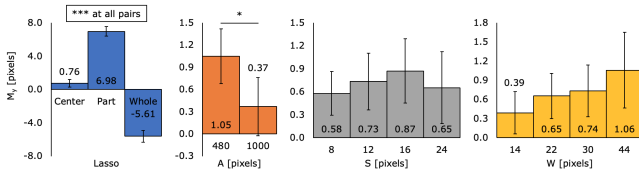


Figure 11. M_y vs. L , A , S , and W .

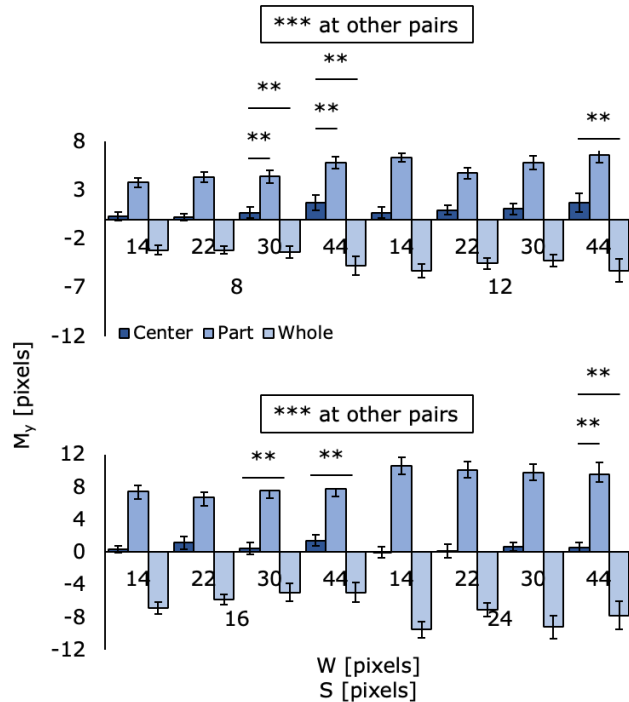


Figure 12. M_y for $Lasso \times S \times W$.

but not those for S ($F_{3,33} = 0.49$, $p = 0.69$, $\eta_p^2 = 0.04$) and W ($F_{3,33} = 0.97$, $p = 0.42$, $\eta_p^2 = 0.08$). Figure 11 shows the results of the post-hoc test. We also observed the interactions for $A \times W$ ($F_{3,33} = 5.26$, $p < 0.01$, $\eta_p^2 = 0.32$), $Lasso \times S$ ($F_{6,66} = 36.67$, $p < 0.001$, $\eta_p^2 = 0.77$), and $Lasso \times S \times W$ ($F_{18,198} = 2.98$, $p < 0.001$, $\eta_p^2 = 0.21$). Regarding $A \times W$, increasing A decreased M_y . Regarding $Lasso \times S \times W$, there were significant differences between $Lasso$ (Figure 12). Figure 13 shows examples of the trajectories that the participants drew, excluding error trials. For example, when $Lasso = Part$, it is shown that the participants drew a stroke on the targets.

Model Fitting

To select a candidate model, we analyzed the speed of the lassoing motion. It is known that the movement of steering through successive objects depends on the margin between objects [17]. For example, when users steer through objects with wide margins, the movement becomes a series of successive crossing motions. In comparison, when the margins are narrow, the movement becomes a single steering motion. Thus, we analyzed the speed of the lassoing motion to confirm whether the participants' movement was crossing or steering motion. In this experiment, the margin (I) between the suc-

Table 1. Model fitting for all $Lasso$ with adjusted R^2 and AIC values ($N = 32$). a and b are estimated regression constants with 95% confidence intervals (CIs) [lower, upper].

$Lasso$	a	b	adj. R^2
<i>Center</i>	-54.7 [-105, -4.00]	40.3 [37.9, 42.7]	0.975
<i>Part</i>	-100 [-142, -57.8]	43.6 [41.6, 45.5]	0.985
<i>Whole</i>	-69.3 [-117, -22.2]	39.5 [37.3, 41.7]	0.978

cessive objects was always 2.04 mm, so, according to [17], the movement was likely to be the steering motion. Figure 14 shows examples of the average speed per 40 pixels. As is shown, the speed did not change sharply, and thus, we believe that the participants' movement was indeed the steering motion. On the basis of the above, we tried to model the lassoing motion through the straight-line path by using the steering law (Equation 2).

As shown in Figure 5, the tolerances are the same between the criteria, i.e., $S + W$. Additionally, because the path amplitude is A , the index of difficulty (ID) is defined as follows:

$$ID = \frac{A}{S + W} \quad (4)$$

Table 1 shows the model fitness for all $Lasso$. For all $Lasso$, the steering law shows good fitting.

Discussions

For the lassoing motion through the straight-line path, as shown in Figures 6 and 8, the movement time and error rate were affected by the path amplitude (A), object size (S), and object vertical margin (W). That is, the lassoing motion was affected by the same factors (i.e., the path amplitude and width) as in the steering operations, and thus, it could be modeled by the steering law. However, there were no significant differences between the lassoing criteria for the movement time and error rate. Additionally, considering the error rate (Figure 8) and standard deviation of the y-coordinate (Figure 9), we can conclude that the lassoing criteria had the same accuracy.

Figure 12 shows that there were significant differences between the lassoing criteria for the mean of the y-coordinate even if the object size and margin were small. That is, Figure 12 shows that the participants could sufficiently understand that the tolerance shifts depending on the lassoing criteria (Figure 5). For example, when the participants use *Center*, they should draw a stroke through the middle between a non-target and target, and thus, the mean of the y-coordinate is close to zero. Because that is shown in Figure 12, we believe that the participants handled the lassoing criteria correctly. Additionally, the participants commented that, when using *Center*, they drew a stroke through the margins between the targets and non-targets, which is also one piece of proof that they could understand the functions of the lassoing criteria.

In summary, this experiment showed the following: (1) the lassoing motion through the straight-line path was affected by the same factors as in the steering operations and can be

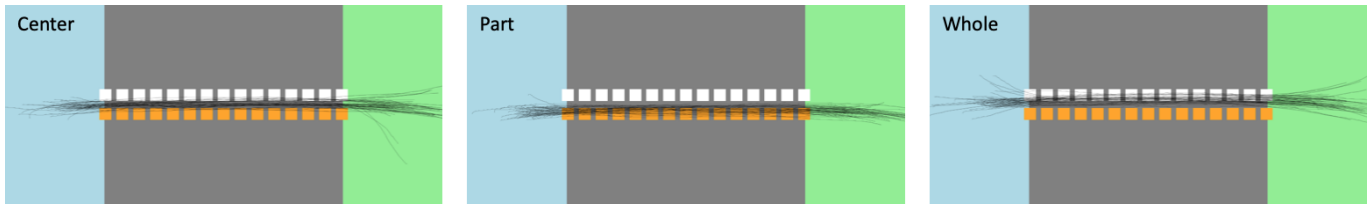


Figure 13. Examples of participants' trajectories for $A = 480$, $S = 14$, and $W = 24$ with each criterion (*Lasso*).

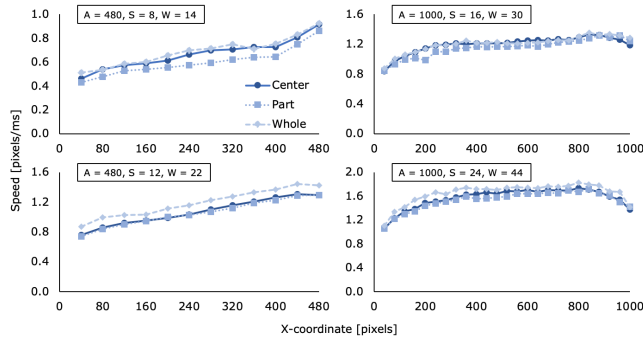


Figure 14. Examples of average speed profile.

modeled by the steering law, but (2) there were no significant differences between the lassoing criteria in terms of movement time and error rate, and (3) the participants handled the lassoing criteria correctly.

EXPERIMENT 2: ONE-LOOP PATH

If we use a task like in Figure 15a, because the amplitude differs depending on the lassoing criteria (Figure 2), we presume that the task completion time will differ depending on the lassoing criteria because of steering through paths with different amplitudes at the same speed (Figure 14). Additionally, if we can model the movement time of such a task, it can be said that we would succeed in modeling the lassoing motion including steering at corners. That is, it can be said that we would succeed in modeling a baseline model of the lassoing motion in consideration of the criteria. In summary, in this experiment, we used a one-loop path task, thereby we evaluated the lassoing criteria and tried to build a baseline model of lassoing motion. We used the same apparatus as in Experiment 1 (Figure 4a) but mostly different participants and others, which we describe below.

Participants

Twelve paid volunteers participated in this study (three women, nine men; age: $M = 22.75$, $SD = 2.05$ years). Three of the people had participated in Experiment 1. All participants were right-handed and operated the stylus accordingly. Each participant received 46 US\$ for the study. Two of the people also participated in Experiment 1.

Task

In this task, there were a blue start bar, a green end bar, white non-targets, and yellow targets (Figure 15a). The center of the path was at the center of the screen. First, the participants crossed the start bar to start the task, they drew a stroke to

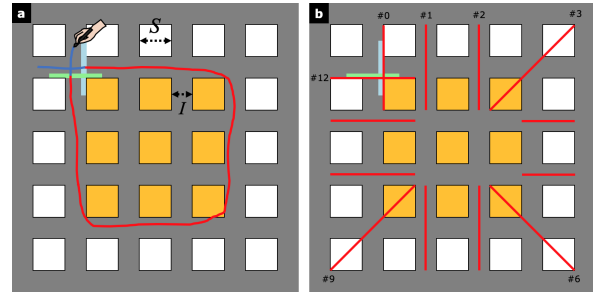


Figure 15. (a) Experiment 2 task outline: participants had to draw stroke to enclose only yellow targets. (b) Checkpoints (red lines) for measuring speed. Note that start bar was No. 0.

enclose all yellow targets, and they crossed the end bar to complete it. After the participants drew the stroke, the system created the selection range by using the stroke from where the start bar was crossed to where the end bar was crossed. Thus, some of the stroke before starting a trial and after finishing it was ignored, i.e., the participants could draw a stroke with enough run-up. If all targets were within the selection range and all non-targets were outside it, a “success” sound was played. Otherwise, a “failure” sound was played, and the trial was regarded as an error. When the trial was a failure, the same task was added to the end of the remaining tasks and reattempted by the participant. After playing either sound, the system changed the colors of the target and non-target borders and displayed those selected and not selected. We asked the participants to confirm whether the trial was a success or a failure; if they did not understand why a trial was considered an error, we instructed them to ask about it. After confirming the trial result, the participants clicked a button and proceeded to the next trial. Additionally, the same as in Experiment 1, if a participant lifted the stylus from the screen, they had to redo it, the object centers were not displayed for all lasso criteria, and the stroke color changed (Figure 15a).

Design

The object size S was 12, 16, or 24 pixels (2.44, 3.26, or 4.89 mm, respectively). The interval I between the objects was 10, 14, or 20 pixels (2.00, 3.00, or 4.00 mm, respectively). Three lasso criteria *Lasso* were considered: *Center*, *Part*, and *Whole* (Figure 1). The numbers of target rows and columns N_{rc} were 3, 5, or 7; when $N_{rc} = 3$, the targets lined up in a 3×3 grid and were enclosed by the non-targets (Figure 15a).

Procedure

The order of working with different criteria *Lasso* was balanced among the 12 participants through a Latin square pattern, and the orders of I , N_{rc} , and S were randomized. One

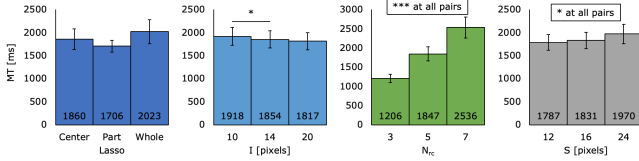


Figure 16. MT vs. I , L , N_{rc} , and S .

set consisted of $3I \times 3N_{rc} \times 3S = 32$ trials. Before starting, each participant was briefed about the experiment and lasso selection. For each *Lasso*, after an introductory practice set, each participant completed five sets to produce experimental data. A total of 4,860 trials (i.e., $3Lasso \times 3I \times 3N_{rc} \times 3S \times 5$ sets \times 12 participants) were conducted, which required approximately 45 min. We asked the participants to take a break if necessary.

Measurements

The dependent variables included the movement time MT (the time from crossing the start bar to crossing the end bar, excluding error trials) and the error rate.

Results

Among the 5,336 trials, 476 errors occurred (8.92%). We analyzed the data by using repeated-measures analysis of variations (ANOVA) and a Bonferroni post-hoc test. The independent variables were *Lasso*, I , N_{rc} , and S , and the dependent variables were the same as those used in the measurements.

Movement Time

We observed the main effects for I ($F_{2,22} = 5.18$, $p < 0.05$, $\eta_p^2 = 0.32$), N_{rc} ($F_{2,22} = 61.73$, $p < 0.001$, $\eta_p^2 = 0.85$), and S ($F_{2,22} = 11.02$, $p < 0.001$, $\eta_p^2 = 0.50$) but not that for *Lasso* ($F_{2,22} = 1.76$, $p = 0.20$, $\eta_p^2 = 0.14$). Figure 16 shows the results of the post-hoc test. We also observed the interactions for $N_{rc} \times S$ ($F_{4,44} = 6.57$, $p < 0.001$, $\eta_p^2 = 0.37$), *Lasso* \times I ($F_{4,44} = 6.41$, $p < 0.001$, $\eta_p^2 = 0.37$), *Lasso* \times S ($F_{4,44} = 11.50$, $p < 0.001$, $\eta_p^2 = 0.51$), *Lasso* \times $I \times S$ ($F_{8,88} = 3.04$, $p < 0.01$, $\eta_p^2 = 0.22$), and *Lasso* \times $N_{rc} \times S$ ($F_{8,88} = 2.45$, $p < 0.05$, $\eta_p^2 = 0.18$). Regarding all interactions, there were no significant differences between *Lasso* (Figure 17).

Additionally, because the total amplitude differs depending on *Lasso* (Figure 2, see *Model Fitting* for details on the amplitude), we also analyzed the average speed [pixels/ms], that is, the value of MT divided by the total amplitude with the same independent values. We did not find significant differences between *Lasso* ($F_{2,22} = 0.20$, $p = 0.82$, $\eta_p^2 = 0.02$; $M = 3.14$, $SD = 0.36$ for *Center*; $M = 2.99$, $SD = 0.23$ for *Part*; $M = 3.12$, $SD = 0.39$ for *Whole*).

Error Rate

We observed the main effects for I ($F_{2,22} = 14.95$, $p < 0.001$, $\eta_p^2 = 0.58$), N_{rc} ($F_{2,22} = 13.47$, $p < 0.001$, $\eta_p^2 = 0.55$), and S ($F_{2,22} = 19.12$, $p < 0.001$, $\eta_p^2 = 0.63$) but not that for *Lasso* ($F_{2,22} = 1.56$, $p = 0.23$, $\eta_p^2 = 0.12$). Figure 18 shows the results of the post-hoc test. We also observed the interaction

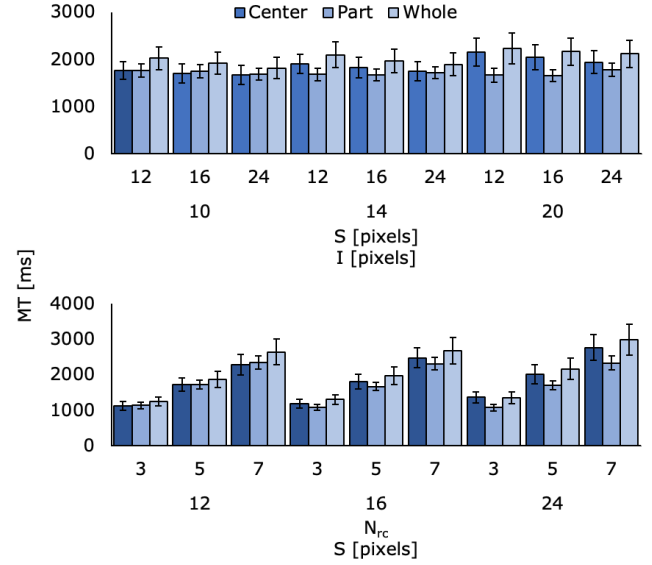


Figure 17. MT for *Lasso* \times $I \times S$ and *Lasso* \times $N_{rc} \times S$.

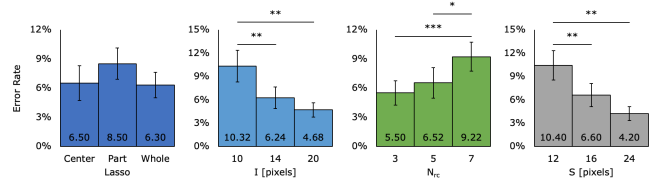


Figure 18. Error rate vs. *Lasso*, I , N_{rc} , and S .

for $I \times S$ ($F_{4,44} = 3.26$, $p < 0.05$, $\eta_p^2 = 0.23$). Increasing I and/or S decreased the error rate.

Subjective Evaluation

After this experiment, we asked the participants how easy the operations were for each criterion on a 5-step Likert scale (1: disagree, 3: neutral, 5: agree). We analyzed the data by using a non-parametric Friedman test with *Lasso* as the independent variable. As a result of analysis, there were no significant differences ($\chi_2^2 = 3.38$, $p = 0.18$, Figure 19). The participants' preferences varied, e.g., some liked the faster but less accurate method, others liked the slower but more accurate method.

Model Fitting

First, we analyzed the speed of the lassoing motion when using *checkpoint* method [16] for selecting candidate models. For

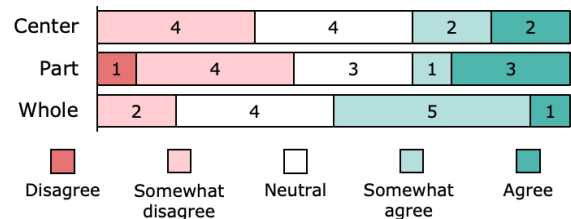


Figure 19. Likert-scale responses to “how easy were the operations for each criterion” ($N = 12$).

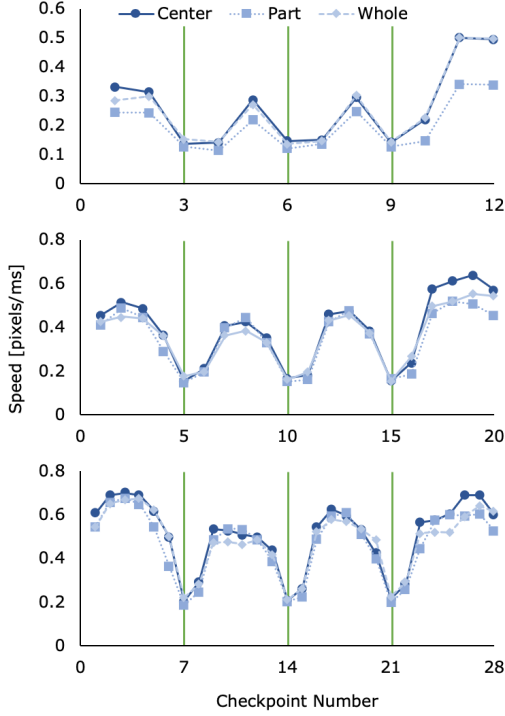


Figure 20. Examples of average speed profile (green lines indicate checkpoints at corners).

example, when $N_{rc} = 3$, we set the checkpoints as shown in Figure 15b and measured the speed from when the participants crossed one red line to when they crossed another red line. Figure 20 shows examples of the average speed profile. We found that the speed from one checkpoint to another had only one peak velocity; the participants' movement was the steering motion, not the series of successive crossing motions. In addition, the speed sharply slowed down at the corners (see the speed on the green lines in Figure 20).

Second, we determined the participants' trajectories (Figure 21). As shown in Figure 21, the participants drew different strokes, and thus, the strokes were close to the center in the order of *Part*, *Center*, and *Whole*. This is evidence that the participants steered through different paths as shown in Figure 2 depending on the lassoing criteria.

In summary, the participants' movement was the steering motion, and, on the basis of the results of Experiment 1 (straight-line path task), the steering law is considered as a candidate model. In addition, the speed decreased at the corners; thus, the participants' movement was the stop and go motion [11], and thus, a model in which the steering law is added to Fitts' law is also considered as a candidate model. Moreover, the participants steered through different paths depending on the lassoing criteria, so the amplitude that the models used should be changed depending on the lassoing criteria. For example, when modeling *Lasso = Center*, the movement distance of the first and fourth straight path segments is $N_{rc}I + N_{rc}S - \frac{I}{2}$, that of the second and third path segments is $N_{rc}I + N_{rc}S$, and the tolerance is $I + S$. Thus, the index of difficulty of the "steering

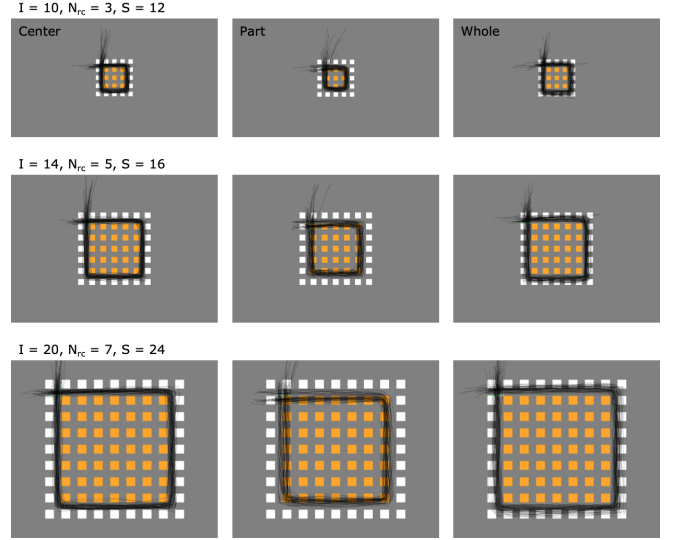


Figure 21. Examples of participants' trajectories for each criterion (*Lasso*).

Table 2. ID_s (steering index of difficulty) and ID_p (pointing index of difficulty) for each criterion.

<i>Lasso</i>	ID_s	ID_p
<i>Center</i>	$4N_{rc} - \frac{I}{I+S}$	$\log_2\left(N_{rc} - \frac{I}{2(S+I)} + 1\right) + 2\log_2(N_{rc} + 1)$
<i>Part</i>	$4N_{rc} + \frac{2(N_{rc}-2)I}{I+S} - 3$	$\log_2\left(N_{rc} + \frac{1}{2}\right) + 2\log_2\left(N_{rc} + \frac{(N_{rc}-2)I}{I+S}\right)$
<i>Whole</i>	$4N_{rc} + \frac{4S}{I+S} - 1$	$\log_2\left(N_{rc} + \frac{S}{I+S} + \frac{1}{2}\right) + 2\log_2\left(N_{rc} + \frac{S}{I+S} + 1\right)$

model" (Table 3) can be written as follows:

$$\begin{aligned}
 ID_s &= \frac{2(N_{rc}I + N_{rc}S - \frac{I}{2}) + 2(N_{rc}I + N_{rc}S)}{I + S} \\
 &= 4N_{rc} - \frac{I}{I + S}
 \end{aligned} \tag{5}$$

Movement around the corners is the stop and go motion, and thus, the "steering model with pointing" (Table 3), which considers the stop and go motion, has an index of difficulty for the pointing in addition to ID_s . ID_p can be written as follows:

$$\begin{aligned}
 ID_p &= \log_2\left(\frac{N_{rc}I + N_{rc}S - \frac{I}{2}}{I + S} + 1\right) \\
 &+ 2\log_2\left(\frac{N_{rc}I + N_{rc}S}{I + S} + 1\right) \\
 &= \log_2\left(N_{rc} - \frac{I}{2(S+I)} + 1\right) + 2\log_2(N_{rc} + 1)
 \end{aligned} \tag{6}$$

Modeling other criteria similarly, we obtain Table 2.

As shown in Table 3, which shows the fitness of the two models for all *Lasso*, all models showed good fitting. However, the steering model has two constants, and the steering model with pointing has three. Because the steering model with pointing is an incremental version of the steering model, generally speaking, it definitely shows a higher R^2 . Thus, we compared Akaike Information Criterion (*AIC*) [4] in addition to R^2 . A model that shows a good fit shows a higher R^2 and lower *AIC* [13, 16], and it is sufficient that the difference between

Table 3. Model fitting for all *Lasso* with adjusted R^2 and AIC values ($N = 27$). a , b_s , and b_p are estimated regression constants with 95% confidence intervals (CIs) [lower, upper].

<i>Lasso</i>	Model	Equation	a	b_s	b_p	adj. R^2	AIC
<i>Center</i>	Steering	$MT = a + b_s ID_s$	283 [74.8, 482]	80.7 [70.6, 90.8]		0.919	358
	Steering with pointing	$MT = a + b_s ID_s + b_p ID_p$	797 [-1233, 2828]	106 [4.97, 208]	-135 [-666, 396]	0.920	359
<i>Part</i>	Steering	$MT = a + b_s ID_s$	474 [410, 539]	62.3 [59.3, 65.3]		0.987	304
	Steering with pointing	$MT = a + b_s ID_s + b_p ID_p$	602 [193, 1012]	69.6 [46.5, 92.6]	-36.1 [-150, 77.9]	0.987	305
<i>Whole</i>	Steering	$MT = a + b_s ID_s$	55.2 [-101, 212]	93.0 [85.9, 100]		0.968	338
	Steering with pointing	$MT = a + b_s ID_s + b_p ID_p$	783 [-969, 2534]	124 [49.3, 199]	-176 [-598, 246]	0.969	340

AIC values is over two [5]. As shown in Table 3, for all *Lasso*, the steering model can sufficiently predict the movement time.

Discussion

In Experiment 1, increasing S decreased the movement time (Figure 6); however, in Experiment 2, increasing S increased the movement time (Figure 16), i.e., S in Experiments 1 and 2 produced opposite effects. Because the task in Experiment 2 was a one-loop path, increasing the object size (S) increased not only the tolerance but also the amplitude at the same time. In comparison, in Experiment 1, because the number of the objects was controlled by A , increasing the object size increased the tolerance but not the amplitude. That is, S affected the path amplitude in only Experiment 2, and thus, results such as those in Figure 16 were obtained.

As shown in Table 3, the steering model with pointing did not show significantly better fitting. According to Pastel's study [11], when the path width is narrow, the motion becomes stop and go. In this experiment, the path width was somewhat wide ($S + I$), and, as shown in Figure 20, the participants' movement did not stop completely, i.e., the speed decreased to approximately 40% of the peak speed. Thus, we believe that the pointing term did not contribute to improving the fitness.

SUMMARY OF TWO EXPERIMENTS

The lassoing operations consisted of steering through a straight-line path and turning at a corner. In this study, we conducted two experimental tasks, i.e., steering through straight-line and one-loop paths, and we found that our results can be modeled on the basis of the steering law. Of course, the application of our current model is limited to straight-line and one-loop paths. However, succeeding in modeling a straight-line path and path with a corner means that it is possible to model lassoing motions through any grid paths. That is, in this study, we succeeded in modeling a baseline model for lassoing motions in consideration of the criteria.

In addition, we found that the movement time, error rate, and subjective evaluation had no significant differences between *Lasso*. Thus, we believe that the ease of use of and the performance of *Lasso* were consistent. As shown in Figures 1 and 2, the path amplitude and objects to be selected differed

depending on the lassoing criteria. Moreover, in pointing operations, it is known that when an area in which click events are fired is unclear, the movement time increases more than when it is clear [14]. When using *Center*, because the width is the interval between the centers between objects, i.e., the width is unclear, we presumed that the movement time would increase. However, we found that the performance and subjective evaluation did not depend on the lassoing criteria.

Because we succeeded in building the baseline model, UI designers can predict the movement time when using the three lassoing criteria under unknown conditions. For example, when $N_{rc} = 9$ (i.e., targets aligned in a 9×9 grid), $S = 18$, and $I = 16$, the designers would obtain 3150 ms for *Center*, 2941 ms for *Part*, and 3506 ms for *Whole*.

LIMITATIONS AND FUTURE WORK

As shown in Figures 14 and 20, we found that there were no significant differences for the speed between *Lasso*. Thus, in selecting multiple objects in a large-scale display [9, 12] (i.e., steering through a path with a long amplitude), it is possible that there will be significant differences for the movement time between *Lasso*.

In this study, we considered a case in which the number of target rows and columns was the same. For example, in a 2×1 grid, users can draw a stroke like in Figure 22. For *Center* and *Part* compared with *Whole*, users can make the stroke around the first and second corners one sharp corner. It is known that users steer through a corner with obtuse or acute angles at a higher speed [11], and thus, in a task like in Figure 22, when using *Center* or *Part*, they may operate faster than that like in Figure 15a.

Our study does not include lassoing operations in more complex conditions, e.g., objects with random sizes, layouts, and shapes. For example, when using *Circle*, the center of a rectangular object is somewhat clear; however, for free form objects, the center is more unclear. In addition, we believe that it would be convenient for a model to include different lassoing criteria because the movement time of other criteria not investigated in this study could be predicted. For example, the movement time for a criterion in which objects of which 80% of their

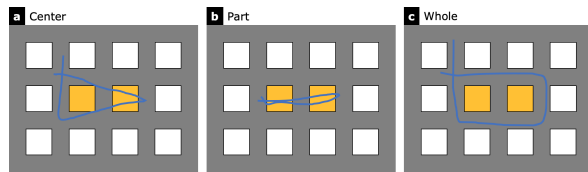


Figure 22. Example of trajectories in 2×1 by (a) Center, (b) Part, and (c) Whole.

area is in the selection range are selected could be predicted. Thus, we will refine our model in further studies.

CONCLUSION

We conducted two experiments in which participants steered through straight-line and one-loop paths by using three lassoing criteria. Our experimental results indicated that the participants handled the lassoing criteria correctly, and they performed the lassoing at an appropriate speed for each path shape. Although the trajectories that the participants drew changed depending on the lassoing criteria, there were no significant differences in terms of movement time, error rate, and subjective evaluation between the criteria. In addition, we successfully constructed a baseline model (i.e., the steering law) to predict the movement time of any of the three criteria. Based on our results, UI designers can select any one of the three criteria. In the future, we will conduct further experiments and refine our model; thereby, we hope that the movement time in lassoing operations can eventually be predicted under any conditions.

REFERENCES

- [1] Johnny Accot and Shumin Zhai. 1997. Beyond Fitts' Law: Models for Trajectory-based HCI Tasks. In *Proceedings of the ACM SIGCHI Conference on Human Factors in Computing Systems (CHI '97)*. ACM, New York, NY, USA, 295–302. DOI: <http://dx.doi.org/10.1145/258549.258760>
- [2] Johnny Accot and Shumin Zhai. 1999. Performance Evaluation of Input Devices in Trajectory-based Tasks: An Application of the Steering Law. In *Proceedings of the SIGCHI Conference on Human Factors in Computing Systems (CHI '99)*. ACM, New York, NY, USA, 466–472. DOI: <http://dx.doi.org/10.1145/302979.303133>
- [3] Johnny Accot and Shumin Zhai. 2001. Scale Effects in Steering Law Tasks. In *Proceedings of the SIGCHI Conference on Human Factors in Computing Systems (CHI '01)*. ACM, New York, NY, USA, 1–8. DOI: <http://dx.doi.org/10.1145/365024.365027>
- [4] Hirotugu Akaike. 1974. A new look at the statistical model identification. *IEEE Trans. Automat. Control* 19, 6 (December 1974), 716–723. DOI: <http://dx.doi.org/10.1109/TAC.1974.1100705>
- [5] Kenneth P Burnham and David R Anderson. 2003. *Model selection and multimodel inference: a practical information-theoretic approach*. Springer Science & Business Media.
- [6] Hoda Dehmeshki and Wolfgang Stuerzlinger. 2010. Design and Evaluation of a Perceptual-based Object Group Selection Technique. In *Proceedings of the 24th BCS Interaction Specialist Group Conference (BCS '10)*. British Computer Society, Swinton, UK, UK, 365–373. <http://dl.acm.org/citation.cfm?id=2146303.2146358>
- [7] Paul M Fitts. 1954. The information capacity of the human motor system in controlling the amplitude of movement. *Journal of experimental psychology* 47, 6 (1954), 381.
- [8] Jakob Leitner and Michael Haller. 2011. Harpoon Selection: Efficient Selections for Ungrouped Content on Large Pen-based Surfaces. In *Proceedings of the 24th Annual ACM Symposium on User Interface Software and Technology (UIST '11)*. ACM, New York, NY, USA, 593–602. DOI: <http://dx.doi.org/10.1145/2047196.2047275>
- [9] David Lindlbauer, Michael Haller, Mark Hancock, Stacey D. Scott, and Wolfgang Stuerzlinger. 2013. Perceptual Grouping: Selection Assistance for Digital Sketching. In *Proceedings of the 2013 ACM International Conference on Interactive Tabletops and Surfaces (ITS '13)*. ACM, New York, NY, USA, 51–60. DOI: <http://dx.doi.org/10.1145/2512349.2512801>
- [10] Sachi Mizobuchi and Michiaki Yasumura. 2004. Tapping vs. Circling Selections on Pen-based Devices: Evidence for Different Performance-shaping Factors. In *Proceedings of the SIGCHI Conference on Human Factors in Computing Systems (CHI '04)*. ACM, New York, NY, USA, 607–614. DOI: <http://dx.doi.org/10.1145/985692.985769>
- [11] Robert Pastel. 2006. Measuring the Difficulty of Steering Through Corners. In *Proceedings of the SIGCHI Conference on Human Factors in Computing Systems (CHI '06)*. ACM, New York, NY, USA, 1087–1096. DOI: <http://dx.doi.org/10.1145/1124772.1124934>
- [12] Florian Perteneder, Martin Bresler, Eva-Maria Grossauer, Joanne Leong, and Michael Haller. 2015. cLuster: Smart Clustering of Free-Hand Sketches on Large Interactive Surfaces. In *Proceedings of the 28th Annual ACM Symposium on User Interface Software & Technology (UIST '15)*. ACM, New York, NY, USA, 37–46. DOI: <http://dx.doi.org/10.1145/2807442.2807455>
- [13] Xiangshi Ren, Jing Kong, and Xing-Qi Jiang. 2005. SH-Model: A Model Based on Both System and Human Effects for Pointing Task Evaluation. *IPSJ Digital Courier* 1 (2005), 193–203. DOI: <http://dx.doi.org/10.2197/ipsjdc.1.193>
- [14] Hiroki Usuba, Shota Yamanaka, and Homei Miyashita. 2018. Pointing to Targets with Difference Between Motor and Visual Widths. In *Proceedings of the 30th Australian Conference on Computer-Human Interaction (OzCHI '18)*. ACM, New York, NY, USA, 374–383. DOI: <http://dx.doi.org/10.1145/3292147.3292150>

- [15] Pengfei Xu, Hongbo Fu, Oscar Kin-Chung Au, and Chiew-Lan Tai. 2012. Lazy Selection: A Scribble-based Tool for Smart Shape Elements Selection. *ACM Trans. Graph.* 31, 6, Article 142 (Nov. 2012), 9 pages. DOI: <http://dx.doi.org/10.1145/2366145.2366161>
- [16] Shota Yamanaka and Wolfgang Stuerzlinger. 2019. Modeling Fully and Partially Constrained Lasso Movements in a Grid of Icons. In *Proceedings of the 2019 CHI Conference on Human Factors in Computing Systems (CHI '19)*. ACM, New York, NY, USA, Article 120, 12 pages. DOI: <http://dx.doi.org/10.1145/3290605.3300350>
- [17] Shota Yamanaka, Wolfgang Stuerzlinger, and Homei Miyashita. 2018. Steering Through Successive Objects. In *Proceedings of the 2018 CHI Conference on Human Factors in Computing Systems (CHI '18)*. ACM, New York, NY, USA, Article 603, 13 pages. DOI: <http://dx.doi.org/10.1145/3173574.3174177>